# Clinical and molecular characterization of novel *POU3F4* mutations in patients with nonsyndromic hearing loss DFN3 and the role of POU3F4 in the development of cochlear lateral wall

Mee Hyun Song

Department of Medicine

The Graduate School, Yonsei University

# Clinical and molecular characterization of novel *POU3F4* mutations in patients with nonsyndromic hearing loss DFN3 and the role of POU3F4 in the development of cochlear lateral wall

Directed by Professor Won-Sang Lee

The Doctoral Dissertation
submitted to the Department of Medicine,
the Graduate School of Yonsei University
in partial fulfillment of the requirements for the degree
of Doctor of Philosophy

Mee Hyun Song

December 2009

This certifies that the Doctoral Dissertation of Mee Hyun Song is approved.

---
Thesis Supervisor

---
Thesis Committee Member

---
Thesis Committee Member

---
Thesis Committee Member

---
Thesis Committee Member

The Graduate School
Yonsei University

December 2009

# ACKNOWLEDGEMENTS

I am truly indebted and thankful to everyone who has helped in the process of completing my dissertation. This dissertation would not have been possible without the support of many people.

I express my sincere gratitude to Professor Won-Sang Lee, the thesis supervisor, who has been my mentor since I began my resident training in Otorhinolaryngology and given continual guidance and support in both academic and psychological aspects. I owe sincere and earnest thankfulness to Professor Jinwoong Bok who has led me through each step during the research with patience and encouragement. I have learned much insight and knowledge in experimental approaches that may interconnect clinical and basic research fields. Special thanks to Professor Un-Kyung Kim for her help in identifying the genetic mutations in the Korean deaf families. Her enthusiasm and expertise in clinical genetics always motivates me to have more academic interest in hereditary hearing loss.

Also, this dissertation would not have been possible without the thoughtful criticisms and intellectual advises from my committee members Professor Jin-Sung Lee and Professor Man-Wook Hur. I would like to express my deepest appreciation to both of them. Thanks to Professor Jae Young Choi who is the one that made me take interest in genetic hearing loss and has given every effort to solve problems that came up unexpectedly. In addition, I give my thanks to Ms. Ling Wu and Ms. Jin Ahn for their technical assistance and dedication which made this work possible and to Mr. Byoung Ki Yoo for his help with histological analysis. Thanks to Professor Taeg Kyu Kwon and Professor Gert Vriend for helping with EMSA and molecular modeling.

I am grateful to my parents who have encouraged me from the start to the end, and also, especially to my loving husband who has stood by my side through the whole time and given endless love and support. Lastly, I thank God for giving me the strength and faith.

# <TABLE OF CONTENTS>

# LIST OF FIGURES

## LIST OF TABLES

<ABSTRACT>

# Clinical and molecular characterization of novel *POU3F4* mutations in patients with nonsyndromic hearing loss DFN3 and the role of POU3F4 in the development of cochlear lateral wall

Mee Hyun Song

*Department of Medicine*
*The Graduate School, Yonsei University*

(Directed by Professor Won-Sang Lee)

X-linked nonsyndromic hearing loss type 3 (DFN3) is caused by mutations in the *POU3F4* locus, which encodes a member of the POU family of transcription factors. Genetic analysis was performed in five Korean families showing clinical characteristics of DFN3 including congenital hearing loss and pathognomonic inner ear anomalies in order to identify novel *POU3F4* mutations in Korean population. To understand how these mutations affect the normal function of the POU3F4 protein, several molecular and cellular *in vitro* analyses were performed. Furthermore, using a mouse model for DFN3, the onset and pattern of the cochlear lateral wall abnormalities were studied in order to identify the role of POU3F4 in inner ear development.

Five different types of novel mutations were identified. The intragenic mutations found in three families caused a substitution (p.R329P) or a deletion (p.S310del) of highly conserved amino acid residues in the POU homeodomain, or a truncation that eliminates both DNA-binding domains (p.Ala116fs). Two families showed deletions in the region of the *POU3F4* gene, in which one deletion was found upstream of the *POU3F4* gene where regulatory elements

are suspected to exist and the other deletion involved almost the whole Xq21 region.

To understand the molecular mechanisms underlying their inner ear defects, the behavior of the normal and mutant forms of the POU3F4 protein was examined in C3H/10T1/2 mesodermal cells. Protein modeling as well as *in vitro* assays demonstrated that the three intragenic mutations are detrimental to the tertiary structure of the POU3F4 protein and severely affect its ability to bind DNA. All three mutated POU3F4 proteins could not transactivate expression of a reporter gene and also failed to inhibit the transcriptional activity of wild type proteins when both wild type and mutant proteins were co-expressed.

Analysis on *Pou3f4*$^{del\text{-}J}$ mutant mice was performed and similar phenotypes were shown as in human X-linked nonsyndromic hearing loss DFN3. Considering the expression pattern of *Pou3f4* during inner ear development, cochlear lateral wall abnormalities were studied by immunohistochemistry and *in-situ* hybridization analysis. All types of otic fibrocytes showed severe defects in *Pou3f4*-deficient mice. In the stria vascularis, normal differentiation of the basal cells could be achieved in the final stages without Pou3f4 function but the process was slightly delayed. Survival and differentiation of the intermediate cells were severely disrupted despite initial differentiation in the mutant mice.

Since most of the mutations reported for DFN3 thus far are associated with regions that encode the DNA binding domains of POU3F4, our *in vitro* studies strongly suggest that the deafness in DFN3 patients is largely due to the null function of POU3F4. In addition, animal model study suggests that *POU3F4* mutation, leading to deafness in DFN3, causes severe developmental defects in the cochlear lateral wall including the otic fibrocytes and stria vascularis, both of which are essential for ionic homeostasis and maintenance of endocochlear potential.

---

Key words : hearing loss, DFN3, POU3F4, inner ear development

# Clinical and molecular characterization of novel *POU3F4* mutations in patients with nonsyndromic hearing loss DFN3 and the role of POU3F4 in the development of cochlear lateral wall

Mee Hyun Song

*Department of Medicine*
*The Graduate School, Yonsei University*

(Directed by Professor Won-Sang Lee)

## I. INTRODUCTION

Fifty percent of congenital hearing loss cases are due to genetic causes, among which X-linked nonsyndromic hearing loss accounts for 1-2%. Of the 4 loci for X-linked nonsyndromic hearing loss (DFN2, DFN3, DFN4, DFN6), the causative gene has only been identified for DFN3, the *POU3F4* gene (Hereditary Hearing Loss Homepage; http://webh01.ua.ac.be/hhh). To date, 11 missense and 5 nonsense mutations in the *POU3F4* gene and more than 15 deletion mutations in the genome encompassing the *POU3F4* upstream regulatory sequence and/or the coding sequence have been identified in DFN3 patients.[1-9] DFN3 accounts for approximately half of the X-linked nonsyndromic hearing loss.[6] Clinical manifestations of DFN3 are X-linked mixed hearing loss and perilymphatic gusher occurring during stapes surgery.[10] However, congenital or progressive sensorineural hearing loss have also been reported.[1-2, 7] Pathognomonic temporal bone deformities, recently classified as incomplete partition type III, have been associated with DFN3, which include fistulous connection between cochlear basal turn and internal auditory canal

(IAC), cochlear modiolar defect, and dilatation of lateral IAC.[11-13] Hearing loss in DFN3 is generally composed of both conductive and sensorineural components. The conductive component is thought to result from anomalies of the oval window and stapedial footplate together with elevated outward pressure of perilymphatic fluid on oval window hindering adequate mobility of the ossicles.[14-15] The sensorineural component invariably shows progression possibly due to the abnormal development of spiral ligament fibrocytes, resulting in alteration of the ion transport system in the inner ear.[5, 16]

The *POU3F4* (*BRN-4, RHS2*) gene (POU domain, class III, transcription factor 4) is a member of the POU family transcription factors that regulate a number of developmental processes.[17] POU family proteins are characterized by a bipartite DNA-binding domain, which is comprised of a 75-amino acid POU-specific domain and a 60-amino acid POU homeodomain tethered by a variable linker of 15~30 residues.[18] The two DNA binding domains are known to make contact with a canonical octameric DNA binding motif, 5'-ATGCAAAT-3', where POU-specific domain cooperates with POU homeodomain to enhance the binding affinity and specificity.[19-20] Thus far, three downstream target genes for POU3F4 have been identified (the proglucagone gene, the D1A dopamine receptor gene, and the involucrin gene), yet its target gene(s) in inner ear is yet to be determined.[21-23]

*POU3F4* gene is expressed in the developing central nervous system and inner ear.[17, 24-25] The otic capsule deformities shown in DFN3 patients are suspected to arise at 25-47 days of gestation in humans, which roughly corresponds to 10.0-13.5 days post coitus (dpc) of mouse development.[26-28] The *Pou3f4* or *Brn-4* gene, the mouse homolog of *POU3F4*, is initially detected in the periotic mesenchyme ventral to the otic vesicle starting from 10.5 dpc which corresponds to the timing when the initial condensation of the periotic mesenchyme begins.[29] At later stages than 11.5 dpc when the entire otic capsule undergoes mesenchymal condensation, *Pou3f4* gene expression is detected

around the entire otic capsule until 13.5 dpc.[29-30] From 15.5 to 18.5 dpc, *Pou3f4* expression was downregulated in the otic capsule and became restricted to prospective otic fibrocytes of the spiral limbus and the spiral ligament.[30] Considering these expression patterns of *Pou3f4*, it is assumed that *Pou3f4* may play a critical role in the morphogenesis of the mesenchymal component of the developing inner ear especially the otic capsule and otic fibrocytes. Two *Pou3f4*-deficient mouse models have been reported, whose inner ear phenotypes closely resemble those of patients with DFN3, which include severe ultrastructural alterations in the cochlear spiral ligament and temporal bone abnormalities with widening of IAC and cochlear anomalies.[16-17] Proper functioning of spiral ligament fibrocytes in the cochlear lateral wall is a prerequisite for normal auditory function because of their role in potassium ion homeostasis that is crucial for maintenance of endocochlear potential.[31]

In this study, five Korean families showing clinical characteristics of DFN3 were identified and genetic analysis revealed 5 different novel mutations in the *POU3F4* gene. To understand how these mutations affect the normal function of the POU3F4 protein, several molecular and cellular *in vitro* analyses were performed. Furthermore, using another type of DFN3 mouse model, the onset and pattern of the otic fibrocyte abnormalities were studied in detail. Results obtained from this study will contribute to the research and clinical fields trying to better understand the pathogenesis of DFN3.

## II. MATERIALS AND METHODS

### 1. Clinical characterizations and genetic analysis of DFN3 families

#### A. Subjects and clinical evaluations

Five Korean families showing congenital hearing loss and characteristic inner ear anomaly of DFN3 were ascertained at the Department of Otorhinolaryngology, Yonsei University College of Medicine. Among these families, 3 families exhibited an X-linked inheritance pattern of hearing loss while 2 other families did not have any family history of hearing loss other than the proband. The proband of each family was subjected to detailed clinical evaluations including medical history, otologic examinations, audiologic testings, and computer-assisted tomography (CT) of the temporal bone. The clinical evaluations were also performed on other members of the families, including affected males and the female carriers. For audiologic testing, either brainstem evoked response audiometry (BERA) or pure tone audiometry (PTA) was performed in line with the age of the patients, and the pure tone average was calculated with the thresholds at 0.5, 1, 2, and 4 kHz. High-resolution temporal bone CT was performed with a 16 row multi-detector CT scanner (SOMATOM Sensation 16; Siemens, Erlangen, Germany) by using a standard temporal bone protocol. Contiguous 0.7-mm scans of the temporal bone were acquired in the axial plane and reformatted coronally with 1.0-mm increments. Written informed consent was obtained from participating individuals, and this study was approved by the Institutional Review Board of the Yonsei University College of Medicine.

#### B. Genetic analyses

For linkage analyses, genomic DNAs from the families were extracted from peripheral blood using the FlexiGene DNA extraction kit (Qiagen, Germany). They were genotyped with centromeric microsatellite marker DXS986 (57.36 cM from Marshfield Map) and telomeric maker DXS6803 (57.91 cM from

Marshfield Map) flanking the DFN3 locus (Xq21.1) using standard PCR conditions. The coding region of *POU3F4* was amplified for direct sequencing using three sets of primers; 1) forward primer 5'-GTAACCCGTGCTAGCGTCTT-3' and reverse primer 5'-GTCGGAGTGATCCTGGCAAT-3'; 2) forward primer 5'-CACTCACCGCACACTAACCA-3' and reverse primer 5'-ACACGCACCACTTCCTTCTC-3'; 3) forward primer 5'-CTCCATCGAGGTGAGTGTCA-3' and reverse primer 5'-GGAGCCAGGAATATGAGATCC-3'. The amplified DNA fragments were sequenced with an ABI PRISM Big Dye Terminator Cycle Sequencing Kit (V3.1) and an ABI PRISM 3130XL DNA analyzer (Applied Biosystems, USA) and data were analyzed by using ABI Sequencing Analysis (v.5.0) and Lasergene- SeqMan software. The resulting sequences were compared with the *POU3F4* sequence from Genbank (Accession No. NM_000307). Seventy Koreans with normal hearing were also sequenced to determine whether the mutations were presented in the unaffected Korean population.

For deletion analysis, PCR amplification was performed with genomic DNA of normal subjects and patients as template. STS markers were selected to amplify the region of interest and additional primer pairs were designed from the non-repetitive unique sequence (http://frodo.wi.mit.edu/, http://www.repeatmasker.org/cgi-bin/ WEBRepeatMasker). Sixty primer pairs were used in this study (primer pairs information is available from the authors on request). PCR reaction was performed as stated above and amplified PCR products were confirmed by direct sequencing reaction.

2. Molecular analysis to identify the effect of *POU3F4* intragenic mutations on normal protein function

A. Subjects

Three Korean DFN3 families identified as having intragenic mutations of

the *POU3F4* gene were included for further molecular analysis.

B. Molecular modeling

The crystal structure of POU2F1/Oct-1 was used as a template to build a model of wild-type and mutant POU3F4 proteins. Modeling was performed with the WHAT IF software[32] with standard parameter settings and protocols as described previously.[33] The details of the modeling protocol, including files used, sequence alignment, parameter choices, etc., are available from http://www.cmbi.ru.nl/~hvensela/pou3f4/.

C. Plasmid construction

To construct expression vectors for wild-type and mutant POU3F4 proteins, the full-length open reading frame (ORF) of the single-exon *POU3F4* gene was amplified by PCR from the genomic DNA of normal or affected males and sub-cloned into the pcDNA3 expression vector. The primer pairs used were 5'-atgaattcatggccacagctgcctcg-3' and 5'-atgcggccgctcagagatcatggcaag-3'. Oligonucleotides encoding the hemagglutinin (HA) epitope were also inserted at the 5' of the *POU3F4* ORF.

D. Immunocytochemistry

C3H10T1/2 cells grown on LabTek 8 chamber slide were transfected with either wild-type or mutant POU3F4 expression plasmids, together with EGFP plasmid. Forty-eight hrs later, the cells were fixed with 4% paraformaldehyde for 10 min and permeabilized by 0.5% Triton for 10 min at room temperature. The cells were then incubated sequentially with monoclonal anti-HA antibody (Zymed, USA) for overnight at 4$^{o}$C, AlexaFluor 568 anti-mouse IgG antibody (Invitrogen, USA) for 1 hrs at room temperature, and DAPI (4', 6'-diamidino-2-phenylindole) for 5 min at room temperature. Images of the immunostained cells were taken with Olympus IX70 fluorescent microscope equipped with Olympus DP70 camera (Zeiss, the Netherlands) and processed using Adobe Photoshop (Adobe Systems, USA). To determine the percentages of the cells expressing POU3F4 proteins outside the nucleus, 100~200 cells

from each chamber were counted manually by an investigator blind to the sample identities. Graphs were plotted based on the numbers collected from at least three independent experiments.

E. Expression and purification of recombinant POU3F4 protein

Glutathione S-transferase (GST) recombinant POU3F4 plasmids were constructed by subcloning the digested fragment containing whole POU3F4 sequences into pGEX-4T-1 *KpnI/EcoRI* sites. Glutathione S-transferase (GST) fusion proteins were purified from the respective *Escherichia coli* BL21 extracts with glutathione-Sepharose (Pharmacia, Piscataway, NY) according to standard procedures.[34]

F. Electrophoretic mobility shift assay (EMSA)

The sequence of the double-stranded oligonucleotide used to detect the DNA-binding activity of POU3F4 was as follows: 5'-CAATATGCTAATCAATATGCTAAT-3'. The reaction mixture for EMSA contained 20 mM Tris-HCl, pH 7.6, 1 mM dithiothreitol, 2 mM $MgCl_2$, 1 mM EDTA, 10% glycerol, 1% NP-40, 1 g poly (dI-dC) and 2 g purified recombinant GST-POU3F4 fusion proteins. For competition assays, unlabeled oligonucleotides were added into the reaction mixture and incubated for 10 min at room temperature. [$^{32}$P]-labeled probe DNA (300,000 cpm) was added, and the binding reaction was allowed to proceed for another 20 min. Mixtures were resolved on 8% non-denaturing polyacrylamide gels at 150V for 4 hrs. Gels were dried and subjected to autoradiography.

G. Transcription reporter assays

The luciferase reporter plasmids were constructed either by inserting the upstream promoter region of human *POU3F4* gene (-482 ~ +25) into the pGL2 basic vector, or by annealing two or three copies of the Pou3f4 binding element (CAATATGCTAAT) into the *Kpn*I/*Bgl*II sites of pNFκB-Luc vector.[35] C3H10T1/2 cells plated in 24-well plates were co-transfected with 300 ng of either wild-type or mutant POU3F4 expression plasmid, or both plasmids

together, 150 ng of the luciferase reporter plasmid, and 20 ng of SV40-renilla plasmid for the transfection efficiency control. The transfected cells were incubated for 24 hrs, and subjected to the luciferase assay according to the manufacturer's protocol (Promega, USA). Transfection efficiencies in each condition were normalized with renilla luciferase activity, which was under the control of a SV-40 promoter. Results were plotted based on at least three independent experiments.

3. Investigation of the role of POU3F4 in the development of cochlear lateral wall using a mouse model

A. Animal model

C3HeB/FeJ-*Pou3f4*$^{del\text{-}J}$/J (The Jackson Laboratory, Bar Harbor, ME, USA) which has a spontaneous deletion of the *Pou3f4* gene was purchased. This mutant strain deficient of the *Pou3f4* gene was reported to have profound deafness and display head shaking and circling behavior. (http://jaxmice.jax.org/strain/004406.html)

B. Deletion analysis of C3HeB/FeJ-*Pou3f4*$^{del\text{-}J}$/J

For deletion analysis, several mouse markers were selected for PCR amplification for genomic DNA of wild type and mutant animals. STS markers were selected to amplify the region of interest and additional primer pairs were designed from the non-repetitive unique sequence (http://frodo.wi.mit.edu/, http://www.repeatmasker.org/cgi-bin/WEBRepeatMasker). The primers used to narrow down the deletion breakpoints are listed in Table 1. PCR reactions were performed and amplified PCR products were confirmed by direct sequencing reaction.

**Table 1. Primers used for deletion analysis**

| Name | Size | Forward primer | Reverse primer |
|---|---|---|---|
| Px-39c6 | 218 | 5'-ACTTGTGTCTAGTTTGTTCTCTCTT-3' | 5'-ATTAGTTGTAGAAGGAAGTACCC-3' |
| m.chm.X 107.542 | 470 | 5'-CAAAGGTCACACCCATAGCAT-3' | 5'-ATAGGCCTCCATCCACTCACT-3' |
| Pou3f4 | 746 | 5'-TGAGTGTCAAGGGCGTACTG-3' | 5'-AGGCGCTGAAAGGTTATTCA-3' |
| m.chm.X 108.071 | 482 | 5'-AGTGTCAGGGGGTGGTAAATC-3' | 5'-CAAAATCCATTTAGGGCCTGT-3' |
| m.chm.X 108.1 | 317 | 5'-AATGGTTCTGAATGGGGTAGG-3' | 5'-CAGCTTGCCTCAAGAAGTGAA-3' |

C. Measurement of auditory brainstem response

Auditory brainstem responses (ABR) were obtained with TDT workstation (Tucker-Davis Technologies, Alachua, FL, USA). ABR testing was conducted in a tailored double-walled sound chamber for animal model. To obtain the ABR, mice were anesthetized by intramuscular injection of tiletamine/zolazepam (30 mg/kg) and xylazine (10 mg/kg), and subdermal electrodes were inserted at the vertex as positive electrode and the ipsilateral ear as reference electrode. The ground electrode was placed on the contralateral ear. Care was taken to attain electrode impedance and difference of interelectrode impedance less than 1 kΩ. Acoustic stimuli evoked by a click were delivered to the animals through ear probes sealed into the ear canal. Body temperature was maintained by placing the mice on a heated warming pad using the heat therapy pump in a soundproof chamber during testing. The sound noise was generated using the same equipment and the click sound was presented at a starting intensity of 80 dB SPL with intensity lowered in decrements of 5 dB SPL until ABR threshold was reached. The recording window was 10 msec and the recorded signals were digitally processed through 60 Hz notch filter and 300-3,000 Hz bandpass filter. ABR threshold was defined as the lowest intensity of stimulation required to attain repeatable ABR wave V.

D. Histologic analysis

After intracardiac perfusion with 4% paraformaldehyde, mice were decapitated and the harvested inner ears were kept in 4% paraformaldehyde overnight at 4˚C. After rinsing with 0.01 M phosphate buffer saline, the specimens were decalcified in 0.5 M EDTA/PBS for 48 hrs, dehydrated with ethanol, and embedded in paraffin. Serial sections of 5 μm thickness were prepared in the mid-modiolar plane and stained with hematoxylin-eosin.

E. Immunohistochemistry

Inner ears of 6 week-old mice were dissected and fixed in 4% paraformaldehyde overnight, decalcified in 0.5 M EDTA/PBS for 48 hrs, then embedded in paraffin wax to be sectioned in 5 μm thickness. The immunofluorescent staining was performed as previously reported.[36] After 1 hr of incubation in a blocking solution (5% normal goat serum in 0.1% Triton X-100 PBS), the tissue sections were incubated with the primary antibodies in the blocking solution for 3 hrs at room temperature. After being washed with 0.1% Triton X-100 in PBS solution three times, the sections were incubated with the corresponding Alexa Fluor 555-conjugated goat anti-rabbit (Zymed, Catalog #A21428) or Alexa Fluor 488-conjugated goat anti-mouse (Zymed, Catalog #A11001) secondary antibodies for 1.5 hrs at room temperature. After completely washing out the secondary antibodies with PBS, the sections were mounted with a fluorescence mounting medium and observed under a confocal laser-scanning microscope. The following primary antibodies and dilutions were used: Rabbit anti-Aquaporin1 polyclonal Ab (1:100, Millipore, catalog #AB3272), rabbit anti-Connexin26 polyclonal Ab (1:400, Zymed, catalog #71-0500), rabbit anti-$Na^+$-$K^+$-ATPase α-1 polyclonal Ab (1:400, Millipore, catalog #06-520), rabbit anti-Kir4.1 polyclonal Ab (1:100, Alomone labs, catalog #APC-035), rabbit anti-Claudin11 polyclonal Ab (Zymed, catalog #36-4500).

F. *In-situ* hybridization

*In-situ* hybridization was performed as described previously.[37] Embryos were fixed overnight with 4% paraformaldehyde in PBS, dehydrated in 30% sucrose, and embedded in Opitimal Cutting Temperature Compound (OCT; Tissue-Tek, Tokyo, Japan). Embryos were sectioned at 12-14 μm thickness onto superfrost slides (VWR Scientific, West Chester, PA, U.S.A) and stored at -80°C. For *in situ* hybridization, slides were first rehydrated, post-fixed, and permeabilized with 10 μg/ml proteinase K for 2 min. Hybridization was carried out in "seal-a-meal" bags (Kapak). Each bag contained 4 slides and 5 ml of hybridization solution with a probe concentration of ~0.2 μg/ml. Details of digoxigenin-labeled riboprobes were obtained from Andreas Kispert, Institut for Molekularbiologie, Hannoever, Germany.[30]

## III. RESULTS

### 1. Clinical characterizations and genetic analysis of DFN3 families

#### A. Clinical manifestations

The pedigree of family SV08-18 showed a typical X-linked recessive inheritance pattern of hearing loss (Fig. 1A). Pure tone audiometric measurements indicated that the proband of this family (IV-2, 6 years) had a severe mixed type of hearing loss (Fig. 1B). Three other affected older males (III-3, 36 years; III-6, 29 years; III-7, 16 years) also showed similar patterns of hearing loss, but the thresholds were higher than that of the proband. Although longitudinal data on hearing loss were not available for these male family members, more severe hearing loss shown in older males especially in the sensorineural component suggested progressiveness of hearing impairment, as previously reported.[5] Two female carriers in the family (III-2, III-4) had normal hearing (Fig 1B).

The second family SV08-17 also showed a typical X-linked recessive inheritance pattern of hearing loss; 5 males being affected in 3 generations (Fig.1A). The proband was diagnosed with severe hearing loss by BERA (thresholds higher than 60 dB nHL (decibel normal hearing level)) one month after birth, and is in the process of auditory rehabilitation with hearing aids. Another affected male in the family (II-4, 23 years) was also diagnosed with hearing loss at the age of 6 years, and developed only limited verbal communication with hearing aids.

In the third family SV08-21, the proband was diagnosed with severe hearing loss by BERA (75 dB nHL and 90 dB nHL on the right and left side, respectively) at the age of 2 years (Fig. 1A). Audiologic testing was not available for other members of the family, although the granduncle of the proband had suspected hearing loss. Since the proband and his mother carried the same mutation, the hearing loss appeared to be inherited in an X-linked

recessive pattern in this family (Fig. 1A).

In the forth family SV08-19, the proband (Ⅲ-6 in Fig. 1A) was first diagnosed with hearing loss at the age of 6 years. There was no family history of hearing loss (Fig. 1A) and the patient did not have any combined medical disease other than hearing loss. Otoscopic finding showed normal drums and no craniofacial abnormalities were observed. His initial audiogram showed mixed type of moderately-severe hearing loss on right side and severe hearing loss on left side. He has used bilateral hearing aids with speech therapy since the initial diagnosis for about 3 years. His audiogram performed at 3 years of follow-up did not show progression of hearing loss. His 37-year-old mother (Ⅱ-8) and 40-year-old father (Ⅱ-9) showed normal hearing level.

In the fifth family SV08-20, the proband (Ⅳ-2 in Fig. 1A) was born at gestational age of 40 weeks weighing 3.98 kg by normal spontaneous vaginal delivery. There was no known family history of hearing loss (Fig. 1A). Otoscopic finding showed middle ear effusion on both sides. No craniofacial abnormalities or dysmorphic features were observed. On BERA performed at 8 months of age, he showed severe hearing loss of 75 dB nHL (decibel normal hearing level) on both sides. He started using bilateral hearing aids at 1 year and 4 months and his speech evaluation showed very limited auditory function. BERA was repeated at 3 years of age and no definitive progression of hearing loss could be seen. Of the family members, audiogram was only available for the child's mother (Ⅲ-2, 30 years) who showed mild high tone loss on both sides. At 8 months of age, he was diagnosed with floppy infant syndrome and central hypotonia requiring intensive physical therapy and rehabilitation process. His brain MRI was normal and electromyography showed no definite evidence of peripheral neuropathy or motor root involvement. He also had vesicoureteral reflux grade V and needed continued use of prophylactic antibiotic treatment.

High resolution temporal bone CT scans were performed on the probands of all five families and on some of the family members. The findings revealed that

the defects of the temporal bones were comparable for all the patients examined, and were characteristic of DFN3,[5, 11] including a wide fistulous connection between the basal turn of the cochlea and the internal auditory canal (IAC), and defects in the cochlear modiolus (Fig. 1C).

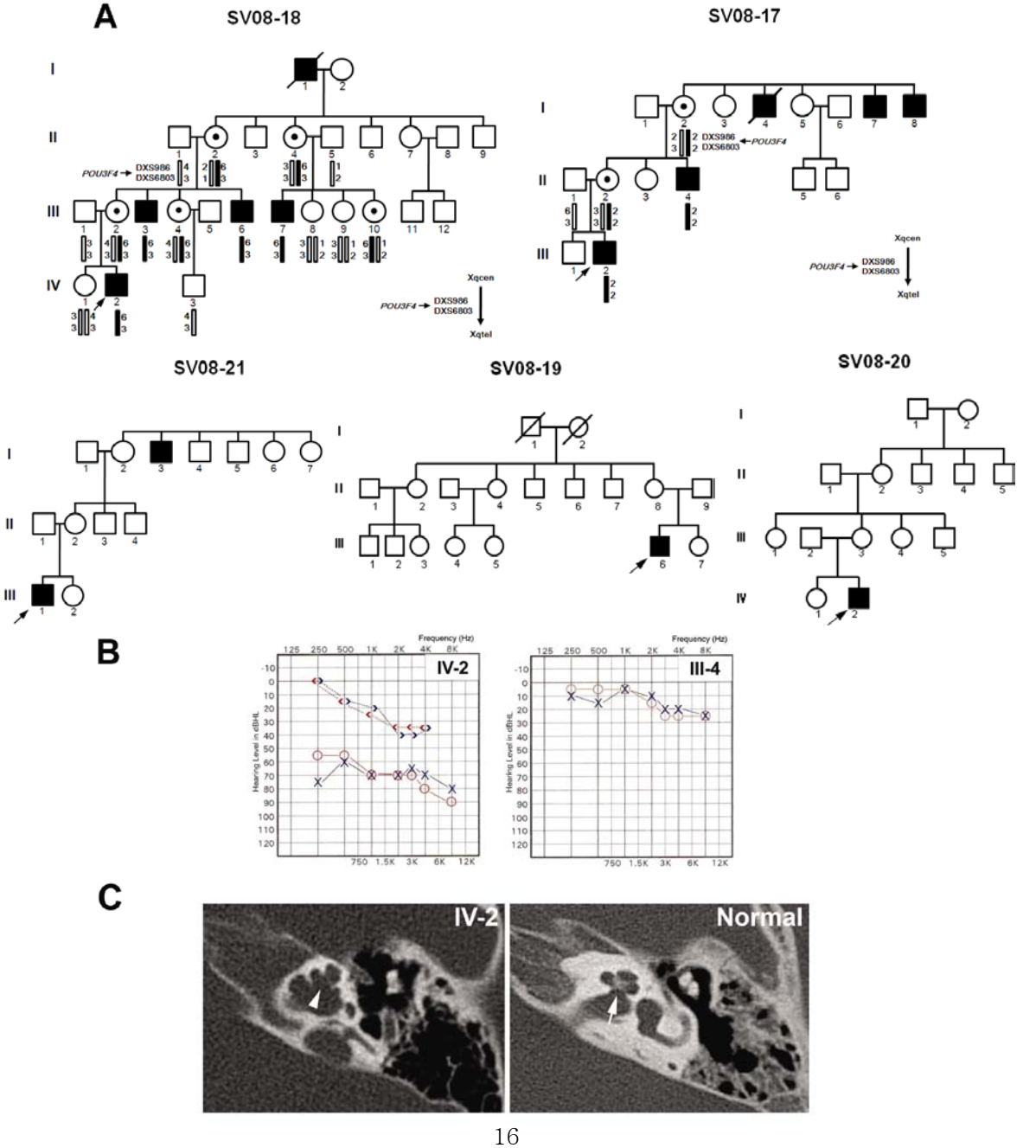

**FIGURE 1.** Pedigrees and clinical characterizations of DFN3 families. (A) Pedigrees of 5 families showing characteristics of DFN3. Families SV08-18 and SV08-17 show a typical X-linked recessive inheritance pattern of hearing loss and the results of linkage analysis are also shown for these 2 families. In family SV08-21, X-linked inheritance was plausible. There was no family history of hearing loss in families SV08-19 and SV08-20. Square (male), circle (female), shaded (affected individual), slashed (deceased), circle with a dot (female mutation carrier), arrow (the proband of the family). (B) A typical audiogram pattern of mixed hearing loss is shown for the proband (IV-2, 6 years) of family SV08-18. A normal audiogram of a female carrier (III-4, 32 years) of the same family is shown for comparison. O (right) X (left): air conduction threshold. < (right) > (left): bone conduction threshold. dBHL: decibel hearing level. (C) High resolution CT scans of the temporal bones of the proband (IV-2) in family SV08-18 shows characteristic findings of DFN3 such as fistulous connection between the basal turn of cochlea and internal auditory canal, and defective cochlear modiolus (Left panel; arrow head), unlike the normal appearance of cochlear modiolus in the normal temporal bone (Right panel; arrow).

B. Linkage and mutation analyses

Since the family histories and clinical evaluations of families SV08-18 and SV08-17 were characteristic for DFN3, we performed linkage analyses using DXS986 and DXS6803 micro-satellite markers and deafness showed linkage to the DFN3 locus in these families (Fig. 1A). Therefore, mutations in the *POU3F4* gene were searched in the affected members of the families by directly sequencing the *POU3F4* coding region. Intragenic *POU3F4* mutations were identified for the 3 families (SV08-18, SV08-17, SV08-21). Sequence analyses in family SV08-18 revealed a point mutation at nucleotide 985, guanine to cytosine (c.986 G>C) (Fig. 2A). This nucleotide change converts an arginine to

a proline at the amino acid position 329 (p.R329P), which is one of the most conserved residues in the POU homeodomain of the POU3F4 protein (Fig. 2E). Sequence analyses of family SV08-17 identified a one base pair (bp) deletion at nucleotide position 346 (c.346delG) (Fig. 2B). This mutation causes a frameshift that encodes 25 new amino acids followed by premature termination of the protein at amino acid position 141 (p.Ala116fs). This results in a truncated form of the POU3F4 protein lacking both DNA binding domains (Fig. 2D; asterisk). The affected members of family SV08-21 had an in-frame deletion of three nucleotides (c.927-929delCTC; Fig. 2C), resulting in a deletion of the amino acid serine (p.S310del) in the POU homeodomain (Fig. 2D).

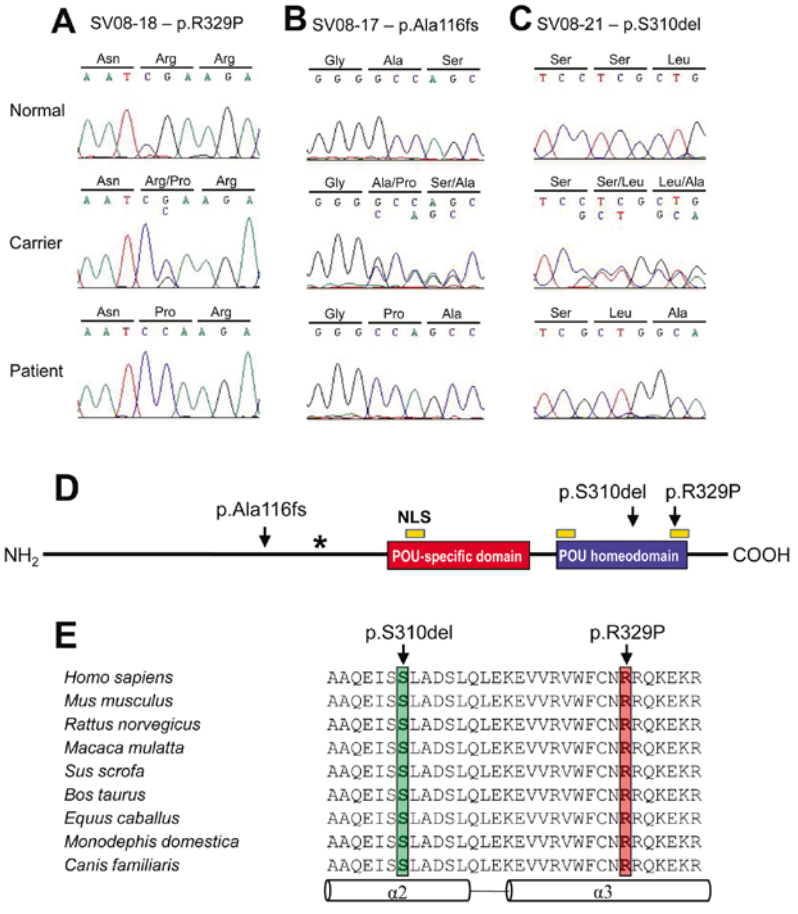

**FIGURE 2.** Three novel mutations in *POU3F4* locus which affect the DNA binding domains of POU3F4 protein. (A-C) Novel mutations identified in three Korean families carrying X-linked hereditary deafness. (D) A schematic illustration of POU3F4 protein labeled with the three novel mutations identified in this study. POU-specific and homeodomain are shown as red and blue boxes, respectively, and three putative nuclear localization signals (NLS) are indicated as yellow boxes above the POU-specific or POU-homeodomain. The positions of the mutation are indicated with arrows, and the location of premature termination in p.Ala116fs mutation is marked by an asterisk. p.R329P mutation is located in one of the putative NLSs in the POU-homeodomain. (E) Alignment of the amino acid sequence of the second and third-helices in the POU3F4 proteins from several animal species. Amino acid sequence in this region is highly conserved in mammals.

For the other 2 families (SV08-19, SV08-20), direct sequencing of *POU3F4* was also performed for identification of mutations. No mutation could be observed in family SV08-19 and *POU3F4* region could not be amplified for patient IV-2 of family SV08-20 (Fig. 3B). Since deletions involving either upstream region of the *POU3F4* gene or the entire *POU3F4* region have been reported to cause phenotypes of DFN3 in previous reports, deletion analysis by PCR amplification of STS markers and several primers was performed in these 2 families. In patient Ⅲ-6 of family SV08-19, the result of PCR reaction showed specific bands for STS markers 81.03 and 82.563 but not for markers 81.515 and 82.560 (Fig. 3B). This result suggested that the deletion was estimated to be between 1 and 1.5 Mb at 200 kb upstream of the *POU3F4* gene for family SV08-19 (Fig. 3A). In patient Ⅳ-2 of family SV08-20, PCR products were obtained for 77.28 and DXS6809, whereas the other primers were not amplified (Fig. 3B). The size of the deletion was estimated to be

approximately 16 Mb which includes almost the entire Xq21 region (Fig. 3A).

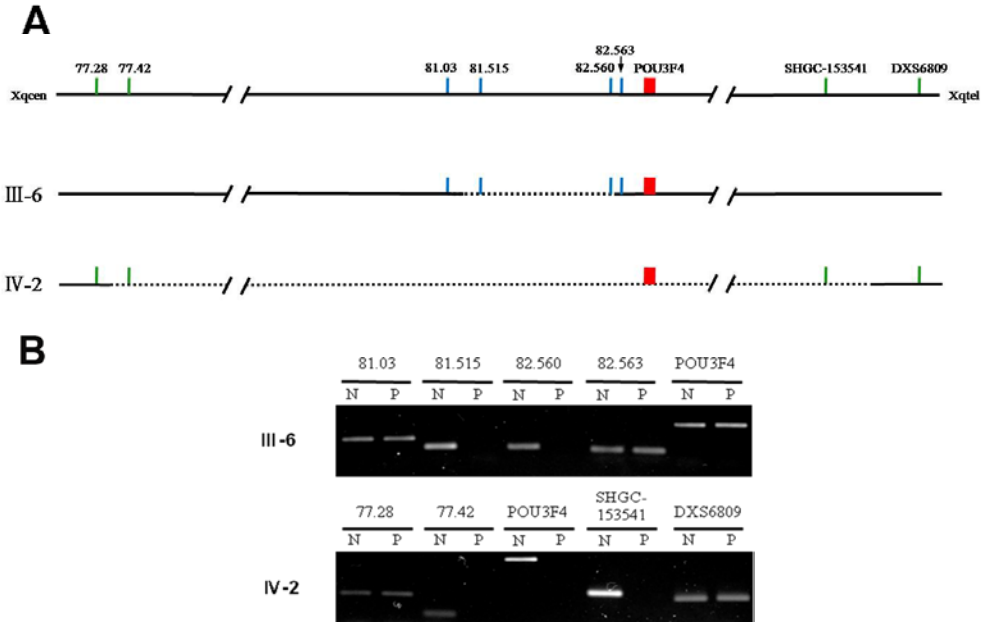


**FIGURE 3.** Characterization of the Xq21 region deletions in families SV08-19 and SV08-20. (A) Schematic representation of genome in the region of deletions. Dotted lines represent the absence of DNA. Primers and physical distances are indicated as bars and numbers above the lines. (B) PCR reactions were carried out for the primers shown with genomic DNA from normal subjects (N) and patients (P).

2. Molecular analysis of *POU3F4* intragenic mutations on normal protein function

A. Structural analyses of wild-type and mutant POU3F4 proteins

The POU3F4 protein consists of an N-terminal domain important for transcriptional activity and two C-terminal DNA-binding domains. These DNA-binding domains consist of the POU-specific domain connected by a

short linker region to the POU homeodomain (Fig. 2D).[24-25] All three mutations identified in this study were expected to affect DNA binding activity of the POU3F4 protein, because they affect one of these domains. To examine the effect of the mutations on the tertiary structure of the POU3F4 protein, molecular models of wild-type, p.R329P and p.S310del POU3F4 proteins were built based on the known crystal structure of the POU2F1/Oct-1 protein.[19]

The p.R329P mutation is located in the third α-helix of the POU-homeodomain, which is crucial for protein-DNA interactions (Fig. 2E, Fig. 4A,B). The substitution of proline for the normal arginine at this position is expected to be detrimental to the α-helix structure due to destabilization of two important salt-bridges as well as loss of a series of hydrophobic contacts. In addition, the amino acid side chain structure of proline typically inserts an obligate bend that disrupts α-helical structures. Such disturbances generally tend to massively reduce the proper protein-DNA interactions.

The serine residue at position 310 is located in the middle of the second α-helix of the POU-homeodomain (Fig. 2E). This helix is not in direct contact with the DNA, but is likely important for the overall structure of the POU-homeodomain. The homology model suggests that α-helical structure will remain after deletion of the serine residue (p.S310del) (Fig. 4C). However, since the absence of one residue will cause a shift of one position for the subsequent residues in this helix, this will have dramatic effects on the stability of this helix because several hydrophobic interactions will get lost and a polar residue will become buried in the hydrophobic core of the protein. As a result, the interaction with the other helices is disturbed and the overall stability of the domain is decreased, which will severely reduce its DNA binding ability.

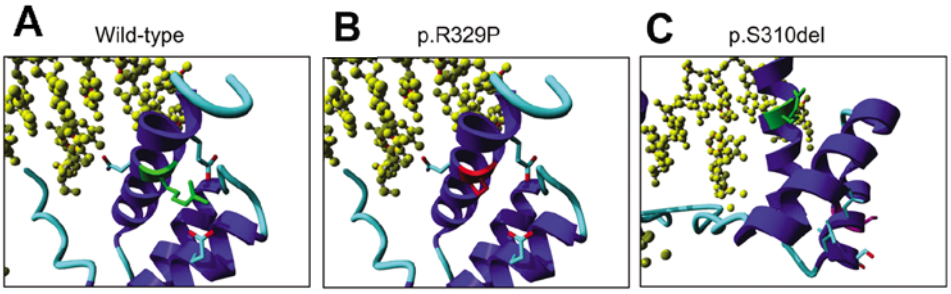


**FIGURE 4.** Molecular modeling of the wild-type and mutant POU3F4 proteins. (A) The third α–helix in the POU-homeodomain is illustrated. The green amino acid residue is Arg329. DNA is shown in a yellow ball-and-stick representation. (B) p.R329P mutation located in the third α-helix of the POU-homeodomain is expected to destabilize the helical structure, affecting the proper protein-DNA interactions. The two glutamates that had an interaction with the lost arginine are shown, as is the asparagine that makes important, specificity relating DNA contacts. (C) In the p.S310del mutant, the lack of one amino acid residue will cause a shift of one position for all subsequent residues, disrupting normal interactions. The details of the modeling are also available from http://www.cmbi.ru.nl/~hvensela/pou3f4/.

B. Effects of *POU3F4* mutations on DNA binding activity

Our modeling study suggested that all three mutations identified in DFN3 patients are likely affecting DNA binding ability by altering the tertiary structure of the DNA binding domains of the POU3F4 protein. To test this possibility, we conducted electrophoretic mobility shift assays (EMSA). Expression vectors encoding wild type and mutant forms of whole POU3F4 protein were constructed, and the proteins were translated *in vitro*. The DNA binding abilities of the *in vitro* translated and purified POU3F4 proteins were tested with the oligonucleotide probe (5'-CAATATGCTAAT-3') that has been

shown to specifically bind the murine Pou3f4 proteins.[35] As shown in Fig. 5A, wild-type POU3F4 proteins bound strongly to the labeled oligonucleotides to form protein-DNA complexes (Fig. 5A, arrow). Specificity of the protein-DNA interaction was confirmed by competition experiments, in which addition of unlabeled oligonucleotide probes completely abolished the protein-DNA interactions. In contrast to the wild-type POU3F4, no detectable protein-DNA complexes were observed with any of the mutant forms of POU3F4. These results indicate that the mutations severely compromise the ability of the POU3F4 proteins to bind target DNA sequences.

C. Effects of *POU3F4* mutations on subcellular localization

The computer program predictNLS[38] predicts three putative nuclear localization signal (NLS) motifs in wild-type POU3F4. One of these is located in the POU-specific domain and the other two are in the POU-homeodomain (Fig. 2D). The p.R329P mutation is located in one of the NLS motifs in the POU-homeodomain, and the p.S310del mutation is located between the two NLSs in the POU-homeodomain (Fig. 2D). The truncating mutation (p.Ala116fs) results in a protein that does not have any of the NLS motifs due to the lack of the DNA binding domains.

To determine how these mutations affect nuclear localization of the POU3F4 proteins, expression vectors encoding wild-type or mutant POU3F4 proteins fused with the HA epitope were transiently expressed in the C3H10T1/2 cells.[39] This mouse mesenchymal cell line was used since *Pou3f4* is mainly expressed in the mesenchyme surrounding the developing inner ear.[29] Immunofluorescent analyses using anti-HA or anti-POU3F4 antibodies showed that wild-type POU3F4 proteins were localized exclusively in the nuclei of transfected cells (Fig. 5B). In contrast, the majority of p.R329P or p.Ala116fs POU3F4 proteins, in which at least one NLS motif is disrupted, were found in both the cytoplasm and the nucleus (Fig. 5B). Although we expected normal nuclear localization for the p.S310del mutant, which preserved all three putative

NLS motifs, POU3F4 proteins with this mutation also lost its normal subcellular localization and was found throughout the cells. This mis-localization could be due to the changes in the tertiary structure of the POU-homeodomain where the NLS domains reside.

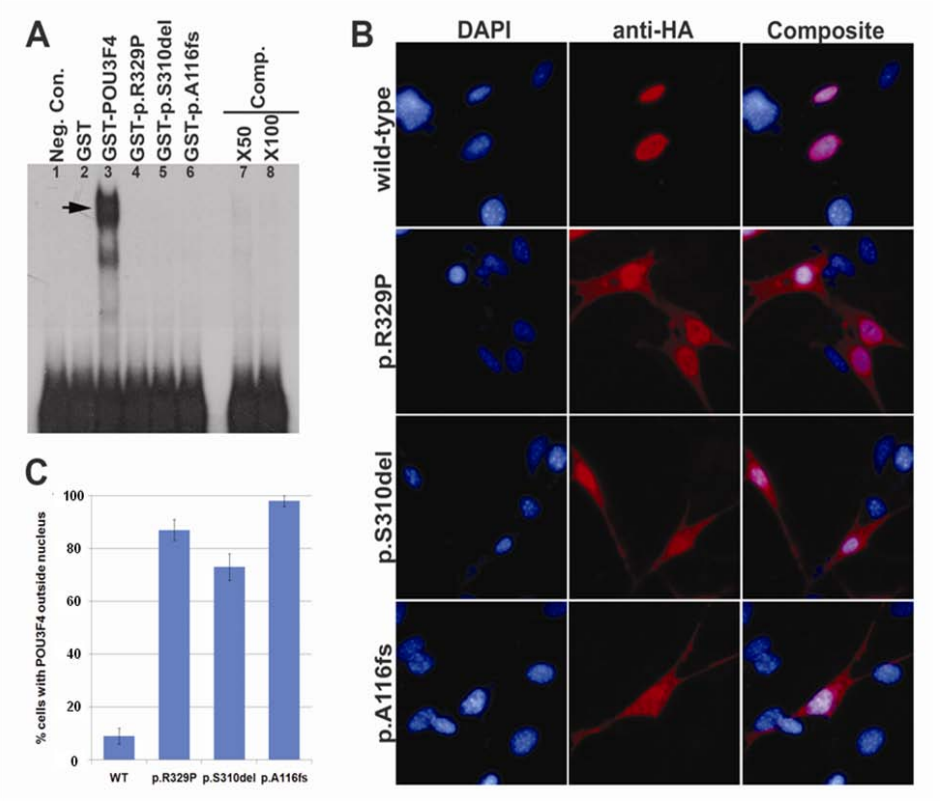


**FIGURE 5.** Disruption of DNA binding ability and subcellular localization by the *POU3F4* mutations. (A) Electrophoretic mobility shift assay (EMSA). Wild-type POU3F4 proteins formed a protein-DNA complex with the labeled oligonucleotides (lane 3; arrow), which were completely disrupted by adding unlabeled oligonucleotides as competitors (lanes 7,8). In contrast, p.R329P (lane 4), p.S310del (lane 5), or p.A116fs (lane 6) mutant proteins failed to bind to the DNA molecules. (B) Immunocytochemical analyses with anti-HA antibody of wild-type and mutant POU3F4 proteins transiently expressed in C3H10T1/2 cells. While wild-type POU3F4 proteins were mostly localized inside the

nucleus, most of the mutant POU3F4 proteins were found in both the nucleus and cytoplasm. (C) A graph quantifying the percentage of cells expressing the POU3F4 proteins outside the nucleus.

D. Effects of *POU3F4* mutations on transcriptional activities

The inability of the mutant POU3F4 proteins to bind to the target DNA sequence or to correctly localize in the nucleus strongly suggested that the transcriptional activity of the mutant POU3F4 proteins would also be severely compromised. To test this, we constructed a reporter plasmid, in which expression of the firefly luciferase gene is regulated by the promoter region (from -472 to +25 bp) of the human *POU3F4* gene, which has been shown to be directly regulated by the POU3F4 protein itself.[35] The reporter plasmid was co-transfected with the plasmid encoding either wild-type or mutant POU3F4 into C3H10T1/2 cells, and the ability of each POU3F4 protein to transactivate the reporter gene was assessed by measuring the luciferase activity in the transfected cells. In this system, wild-type POU3F4 protein activated the reporter gene expression almost three-fold, but all three mutant POU3F4 proteins failed to activate the gene expression (Fig. 6B), indicating that the *POU3F4* mutations completely abolish the transcriptional activity of POU3F4 proteins. Similar effects were observed with another reporter construct, whose luciferase expression is under the control of two or three copies of the POU3F4 recognition element (5'-CAATATGCTAAT-3') (data not shown).[35] Next, we tested to see if the mutant POU3F4 proteins could act as dominant-interfering variants. When both wild-type and any of the mutant POU3F4 proteins were co-expressed, the reporter expression activated by wild type POU3F4 protein was not affected, indicating that the mutant POU3F4 proteins did not inhibit normal transcriptional activity of wild type proteins (Fig. 6B). These results demonstrate that the three mutations identified in the DFN3 patients cause

functional nulls of the POU3F4 protein.

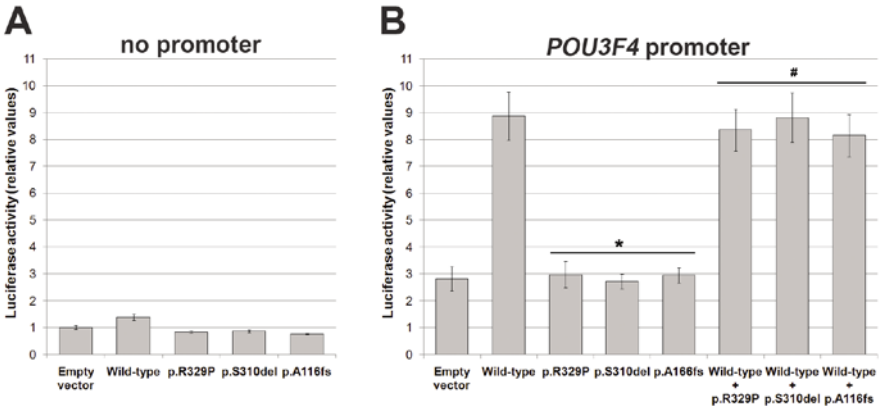


**FIGURE 6.** Transcriptional activity of POU3F4 abolished by the *POU3F4* mutations. (A) Luciferase activities in cells co-transfected with various POU3F4 proteins and the promoter-absent reporter construct (pGL2 basic vector). No luciferase activity was observed in cells expressing either wild-type or mutant POU3F4 proteins. (B) Luciferase activities in cells co-transfected with the reporter construct containing the POU3F4 promoter region (from -472 to +25 bp) and various forms of POU3F4 proteins. Wild-type POU3F4 protein up-regulated the reporter gene expression, while none of the mutant POU3F4 proteins did. Co-transfection of the wild-type and any of the mutants induced luciferase activities comparable to the level activated by the wild-type alone. * Significantly different from wild-type (t-test, $p<0.001$). # Not significantly different from wild-type ($p>0.1$).

3. Investigation of the role of POU3F4 in the development of cochlear lateral wall using a mouse model

A. Deletion analysis of C3HeB/FeJ-*Pou3f4*$^{del\text{-}J}$/J

C3HeB/FeJ-*Pou3f4*$^{del\text{-}J}$/J having a spontaneous deletion of the *Pou3f4* gene was obtained from The Jackson Laboratory (Bar Harbor, ME, USA). This mutant strain is known to have profound deafness and loss of endocochlear

potential.[40-41] (http://jaxmice.jax.org/strain/004406.html) No study has yet been performed with this mouse model to analyze in detail the developmental defects resulting from the absence of *Pou3f4*, although several studies were reported using different mutant strains deficient of *Pou3f4*.[16-17, 42]

Deletion analysis revealed a large deletion that includes the *Pou3f4* gene, spanning a region ranging from 529 kb ~ 570 kb. The deletion breakpoints were approximately 470 kb upstream and approximately 70 kb downstream of the *Pou3f4* gene. Within the deleted region, 3 hypothetical genes were present however none of them were identified to have any association with ear development or hearing loss.

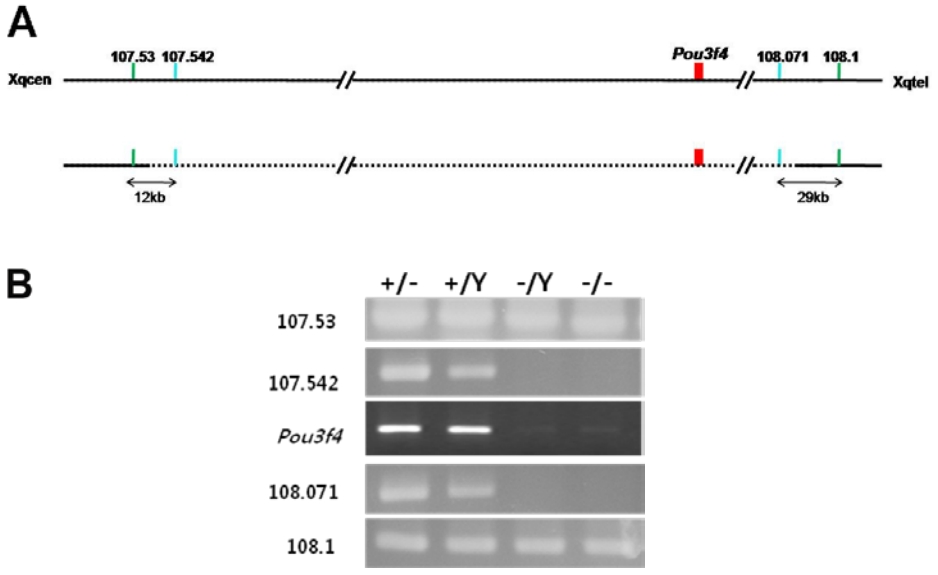


**FIGURE 7.** Deletion analysis of C3HeB/FeJ-*Pou3f4*$^{del\text{-}J}$/J. (A) Schematic representations of mouse genome in the region of deletion. Dotted lines represent the deleted portion of DNA. Primers are indicated as vertical bars and numbers above the bars. The *Pou3f4* gene is presented as a red box. The distances between the 2 primers closest to the deletion breakpoints upstream and downstream of the *Pou3f4* gene are marked respectively. (B) PCR reactions

are shown for the primers used for deletion analysis. +/-: *Pou3f4*$^{+/-}$ female, -/-: *Pou3f4*$^{-/-}$ female, +/Y: *Pou3f4*$^{+/Y}$ male, -/Y: *Pou3f4*$^{-/Y}$ male

B. Auditory threshold measurement

Auditory brainstem response was measured at 3 weeks after birth. All of the controls (*Pou3f4*$^{+/-}$, n=3) showed a click-ABR threshold of 25 dB nHL while in mutant males (*Pou3f4*$^{-/Y}$, n=4), no wave was detectable up to 80 dB nHL, meaning that they were profoundly deaf by 3 weeks of age (Table 2).

**TABLE 2.** Auditory threshold measurement by click-ABR in *Pou3f4*-deficient mice at 3 weeks.

| Mice | Genotype | Number | Click-ABR threshold |
|---|---|---|---|
| Control | *Pou3f4*$^{+/-}$ | n=3 | 25 dB |
| Mutant | *Pou3f4*$^{-/Y}$ | n=4 | No response |

C. Cochlear abnormalities of *Pou3f4*-deficient mice

Cochlear morphology was examined by comparing the mid-modiolar section of 3 week-old control and mutant mice (Fig. 8). The modiolus which is the central bony core of the cochlea was severely defective and the interscalar septum (IS-2) between upper basal turn and upper middle turn was completely missing with flattening of the interscalar ridge (IR-2) (Fig. 8A,8B). Interscalar septum (IS-1) between the lower basal turn and lower middle turn was present but much thicker compared to the control. Scala tympani (ST) of the basal turn was contracted showing smaller volume in *Pou3f4*-deficient mice. The magnified view of the scala media revealed severe abnormalities in the spiral ligament fibrocytes of *Pou3f4*-deficient mice (Fig. 8C,8D). Type IV and V fibrocytes located above the stria vascularis and lateral to the basilar membrane,

respectively, were almost absent. The cell density of type I fibrocytes, underlying the stria vascularis (StV), was decreased and type II fibrocytes, situated under the spiral prominence, appeared to be reduced in volume. The stria vascularis (StV) seemed less densely populated and the normal tight interdigitation between the intermediate cells and marginal or basal cells appeared to be severely decreased in the mutants (arrowheads in Fig. 8E,8F). Cells comprising the Reissner's membrane (RM) were less flattened (arrow in Fig. 8D,8F) in mutant mice compared to the control. The organ of Corti (OC) looked grossly normal on hematoxylin-eosin staining (Fig. 8C,8D).

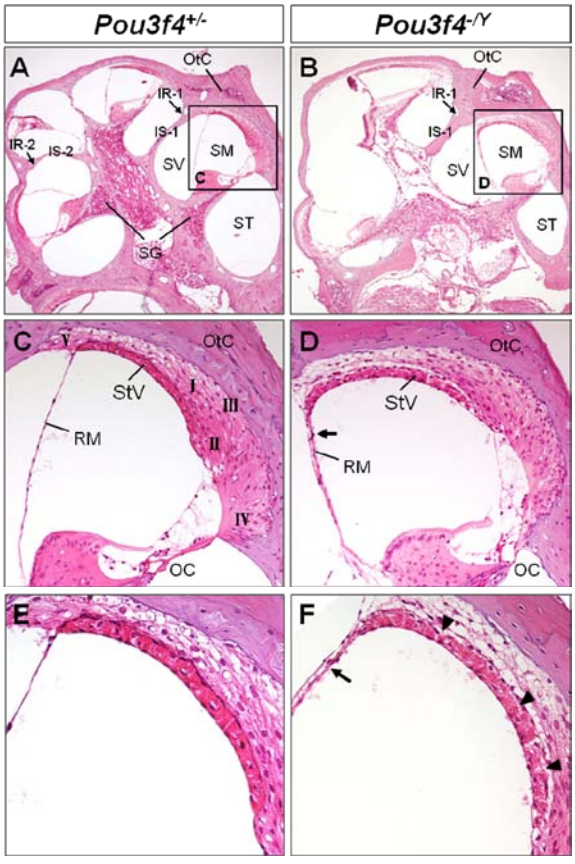


**FIGURE 8.** Histological defects in the cochlea of *Pou3f4*-deficient mice. Hematoxylin-eosin staining of the mid-modiolar sections of the cochlea in

control (A, C) and *Pou3f4*-deficient mice (B, D) at 3 weeks of age. (A, B) Defective modiolus and wide communication between the basal turn of cochlea and internal auditory canal are seen in *Pou3f4*-deficient mice compared to the control. Interscalar septum-2 (IS-2) is completely missing as well in the mutant mice. (C, D) Magnified view of the scala media and cochlear lateral wall. Type I, II, IV, V fibrocytes of the spiral ligament show defects in the mutant mice while organ of Corti appear relatively intact. Stria vascularis (StV) seems less densely populated and Reissner's membrane (arrow in Fig. 8D,8F) is thicker in the mutant mice. (E, F) Magnified view of the stria vascularis. Normal tight interdigitation between the intermediate cells and marginal or basal cells appears to be severely decreased in the mutants (arrowheads in Fig. 8F).
*IR*, interscalar ridge; *IS*, interscalar septum; *OC*, organ of Corti; *OtC*, otic capsule; *RM*, Reissner's membrane; *SM*, scala media; *ST*, scala tympani; *StV*, stria vascularis; *SV*, scala vestibule

D. Defects of otic fibrocytes and stria vascularis in *Pou3f4*-deficient mice

Immunohistochemistry using various markers for each type of fibrocytes and different cell types of stria vascularis was performed to further characterize the identified histologic defects in P42 *Pou3f4*-deficient mice. Na-K-ATPase is an ion channel that is expressed in type II, IV, V fibrocytes as well as on the basal surface of marginal cells of stria vascularis.[43] In the control, the normal expression was identified whereas in the mutant mice, expression at type IV, V fibrocytes was nearly abolished and the volume of type II fibrocytes was significantly reduced (Fig. 9A, 9B). However, Na-K-ATPase expression at the stria vascularis was intact demonstrating normal differentiation and localization of marginal cells in stria vascularis. Connexin26 which is a gap junction important for maintenance of ion homeostasis showed strong expression in type I and V fibrocytes as well as at basal cells of stria vascularis in the control (Fig.

9C).[43] In mutants, Connexin26 expression at type I and V fibrocytes was completely lost while normal expression was seen at the region lining the basal cells of stria vascularis (Fig. 9D). Expression of aquaporin1, a marker for type III fibrocytes, which normally lines the otic capsule was decreased and dispersed into type I and II fibrocyte area (Fig. 9E, 9F).[44] Interestingly, when fibrocyte defects were investigated further at P21, aquaporin1 expression of the control exhibited a dispersed pattern very similar to that of the mutant instead of being localized to the otic capsule lining (Fig. 10A-D). This may suggest that proper localization and differentiation of type III fibrocytes is lost after P21 in *Pou3f4*-deficient mutants. For connexin26, no significant difference could be noted between P21 and P42 results (Fig. 10E-H).

To test the integrity of intermediate and basal cells of stria vascularis, Kir4.1 and Claudin11 were used as markers, respectively.[45-46] Kir4.1 which is an inwardly-rectifying potassium channel located at apical surface of intermediate cells, showed significantly weaker signals in mutant mice compared to the control although the expression pattern was similar (Fig. 9G, 9H). Claudin11, specific for basal cells of stria vascularis, was normally expressed in the basal cell region similar to the control (Fig. 9I, 9J).

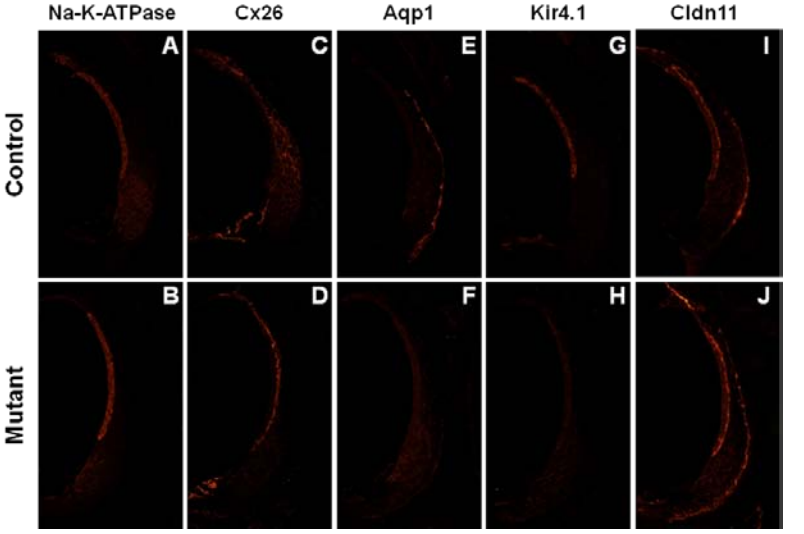


**FIGURE 9.** Immunofluorescence of otic fibrocytes and stria vascularis at P42. Detection of markers for otic fibrocytes and stria vascularis on midmodiolar sections of cochlea of control and mutant mice at P42. (A-J) Severe defects were noted for all types of otic fibrocytes and intermediate cells of stria vascularis. *Na-K-ATPase* (Type II, IV, V fibrocytes, marginal cells), *Cx26* (Connexin26; Type I, V fibrocytes, basal cells), *Aqp1* (Aquaporin1; Type III fibrocytes), *Kir4.1* (Inwardly-rectifying potassium channel; Intermediate cells), *Cldn11* (Claudin11; Basal cells)

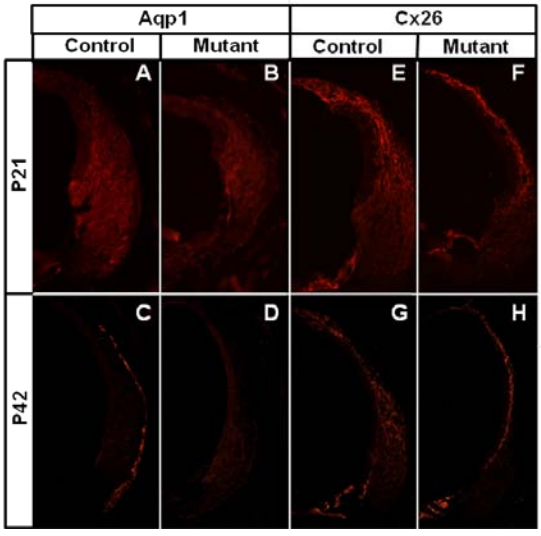


**FIGURE 10.** Expression patterns of aquaporin1 and connexin26 at P21 and P42. Immunofluorescence of aquaporin1 (A-D) and connexin26 (E-H) was compared at stages P21 and P42. At P21, aquaporin1 expression of the control exhibited a dispersed pattern very similar to that of the mutant instead of the being localized to the otic capsule lining (A,B). At P42, type III fibrocytes become localized to the bony lining of otic capsule in the control, while the expression decreases and remains dispersed in the mutant (C,D). For connexin26, no significant difference could be noted between P21 and P42 results (E-H).

The 3 cell types comprising the stria vascularis are derived from different origins. The marginal cells and intermediate cells are derived from neuroectoderm and neural crest, respectively, whereas the basal cells are thought to be differentiated as a result of mesenchymal-epithelial transition from the condensing mesenchymal cells underneath the stria.[30, 47] From the results of hematoxylin-eosin staining (Fig. 8C, 8D) and immunofluorescence (Fig. 9G, 9H), defect of stria vascularis was highly suspected. Therefore, developmental abnormalities of stria vascularis were examined further by

*in-situ* hybridization from E18.5 to P5. First, expression of the marginal cell marker, *Bsnd* encoding chloride channels on the basolateral membrane of the marginal cells, was assessed which showed nearly normal pattern in the mutant compared to the control (Fig. 11A,11B,11E,11F,11I,11J).[48] *Trp2*, which is an intermediate cell marker, showed similar expression pattern in the mutant as the control, however, the distribution was more scattered and dispersed beneath the marginal cells suggesting more delayed differentiation and localization of the intermediate cells compared to the control (Fig. 11C,11D,11G,11H,11K,11L).[49]

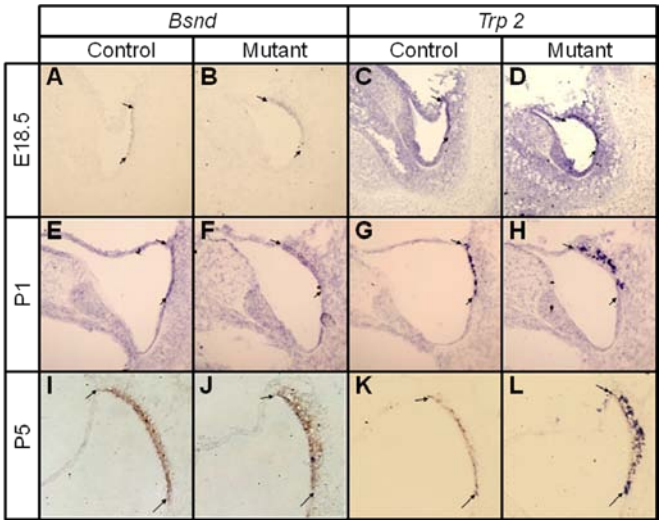


**FIGURE 11.** Developmental abnormalities of stria vascularis in *Pou3f4*-deficient mice. *In-situ* hybridization of markers for marginal and intermediate cells of stria vascularis in mutant and control mice from E18.5 to P5. (A-L) Markers for marginal cells (*Bsnd*) and intermediate cells (*Trp2*) are detected at areas of prospective stria vascularis in both mutant and control mice however, the distribution of *Trp2* is more scattered and dispersed suggesting delayed differentiation and organization in the mutant compared to the control. Arrows (Borders of stria vascularis), *Bsnd* (Barttin; marginal cells), *Trp2* (Intermediate cells)

Although immunofluorescence of Cldn11, a marker for basal cells of stria vascularis, showed no definitive evidence suggesting defect of the basal cells in the mutant, abnormalities in the basal cell differentiation requiring proper condensation and functioning of mesenchymal compartment could be suspected in *Pou3f4*-deficient mice since *Pou3f4* is expressed in the otic mesenchyme of cochlear lateral wall throughout development of the inner ear. To find out whether mesenchymal cells undergo proper condensation and epithelial transition to form intact basal cells in the absence of functioning Pou3f4, the expressions of connexin26 and E-cadherin, both of which are known to be expressed in the condensing mesenchyme underneath the developing stria vascularis, were examined.[30] Normally, connexin26 is expressed in the condensing mesenchyme underneath the stria until P10 when mature strial basal cells begin to function and after this period, its expression is found mainly at type I and V otic fibrocytes in the lateral wall.[43] At E18.5, mesenchymal condensation, marked by the expression of *Cx26* and *E-Cad* was detected in the location of prospective stria vascularis in the control whereas no signal was detected in the mutant (Fig. 12A-D). At P1, mesenchymal condensation began to occur in the mutant, however, the distribution was much more dispersed and disorganized in the mutant as compared to the control (Fig. 12E-H). At P5, *Cx26* and *E-Cad* became restricted to the basal cell region of stria vascularis in the control whereas in mutants, mesenchymal cells were still in the process of condensation suggesting a delay in differentiation of basal cells (Fig. 12I-L).

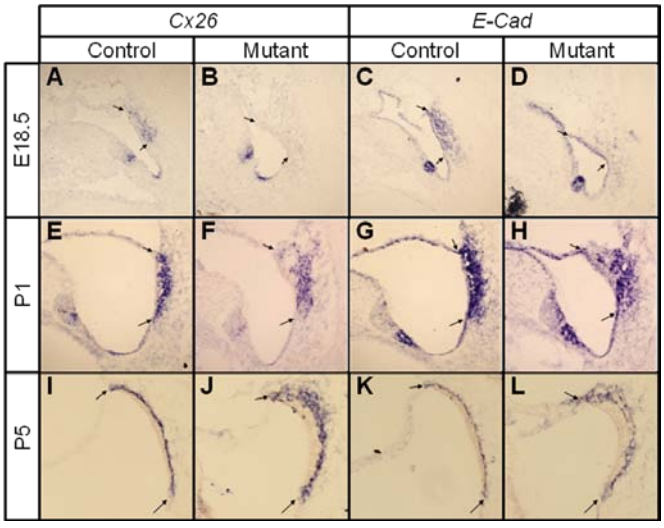


**FIGURE 12.** Mesenchymal condensations underneath the stria vascularis for basal cell differentiation in *Pou3f4*-deficient mice. *In-situ* hybridization of markers known to be expressed in mesenchymal condensates underneath the developing stria vascularis in mutant and control mice from E18.5 to P12. (A-L) At E18.5, mesenchymal condensation, marked by the expression of *Cx26* and *E-Cad* is detected in the location of prospective stria vascularis in the control (A,C) whereas no signal is detected in the mutant (B,C). At P1, mesenchymal condensation begins to occur in the mutant however, the distribution is much more dispersed and disorganized in the mutant (F,H) as compared to the control (E,G). At P5, *Cx26* and *E-Cad* becomes restricted to the basal cell region of stria vascularis in the control (I,K) while in mutants, mesenchymal cells still show a dispersed pattern (J-L). *Cx26* (Connexin26), *E-Cad* (E-Cadherin)

Concerning the development of the stria vascularis, the above results suggested that nearly normal differentiation of marginal and basal cells of the stria vascularis was eventually achieved in the absence of the *Pou3f4* gene, nevertheless a delay in the developmental process was inevitable. As for the

intermediate cells, delayed cytodifferentiation as well as defective differentiation or survival in the final stages of the development leading to decreased cellular density of intermediate cells in the adult stria vascularis was suspected. Since intermediate cells of stria vascularis play an important role in the generation and maintenance of endocochlear potential,[50] it is believed that defects in the otic fibrocytes together with the abnormalities in the stria vascularis collectively contribute to the absence of endocochlear potential and deafness in the *Pou3f4*-deficient mice.

## IV. DISCUSSION

Five novel mutations of the *POU3F4* gene were identified in Korean families showing characteristics of X-linked nonsyndromic hearing loss DFN3. To date, more than 30 mutations in the region of *POU3F4* have been reported to be related to DFN3 however, only few reports deal with mutations found in the Asian population.[5, 51-52] In Koreans, 2 intragenic mutations have been discovered recently whereas deletion mutations involving upstream of or encompassing the *POU3F4* gene have never been reported.[52] In this study, 3 of the mutations were found within the *POU3F4* gene in which there were 1 missense mutation of the POU-homeodomain (p.R329P), 1 single base pair deletion causing frameshift followed by premature termination (p.Ala116fs), and lastly, 1 in-frame deletion causing deletion of a single amino acid (p.S310del). In 2 families, deletions in the region of the *POU3F4* gene were identified. One deletion was found upstream of the *POU3F4* gene where regulatory elements are suspected to exist and the other deletion involved almost the whole Xq21 region.[8] The clinical manifestations of the families revealed similar characteristics; especially the temporal CT findings were remarkably analogous showing minimal inter- and intra-familial variability despite the differences in mutation types among the 5 families. The audiologic features showed some variability although clear genotype-phenotype correlation could not be identified. More data collection in Korean population will be needed to clarify any specific traits that may be related to differences in ethnic backgrounds.

POU3F4 protein is a transcriptional factor comprised of two DNA-binding domains, the POU-homeodomain and the POU-specific domain.[25] Like the three intragenic mutations found in this study, most of the *POU3F4* mutations identified in DFN3 patients specify amino acid changes in regions that encode the DNA binding domains, the majority being in the POU homeodomain,[5] suggesting that loss of DNA binding ability may be a common pathological

mechanism at the molecular level. Indeed, protein modeling and several molecular analyses demonstrate that the *POU3F4* mutations severely disrupt the DNA binding ability of POU3F4 thereby, completely abolishing the transcriptional activity of the protein. The mutant POU3F4 proteins failed to inhibit normal transcriptional activity of wild-type POU3F4, excluding the possibility that the mutant proteins act as dominant-interfering variants. Overexpression of the mutant POU3F4 proteins in C3H10T1/2 cells did not seem to have any obvious deleterious effects on normal cell behaviors such as cell proliferation or cell death (data not shown). Together, these observations strongly suggest that the hearing loss in DFN3 is caused by the loss of function of POU3F4 protein, rather than by gain of ectopic functions of mutant proteins. Clinical evaluations of DFN3 patients in this study are consistent with previously published reports that demonstrated no clear genotype-phenotype correlation between the different types of the *POU3F4* mutations and the inner ear.[53]

The hearing loss in DFN3 by *POU3F4* mutations is most likely associated with lack of expression of downstream target gene(s) that plays critical roles in inner ear development, especially in the mesenchymal remodeling and otic epithelial-mesenchymal interactions. Only a few target genes of POU3F4 have been identified to date in other tissues; proglucagon gene in the α-cells of the pancreas,[21] D1A dopamine receptor gene in the striatum,[22] and human involucrin gene in the epidermis.[23] However, little is known about downstream targets of POU3F4 in the peri-otic mesenchyme where *POU3F4* is actively expressed.[29] The temporal bone CT scans of DFN3 patients as well as the *Pou3f4* knockout inner ear phenotypes suggest that most of the inner ear malformations were found in the structures derived from the mesenchyme.[16-17] In the earlier embryonic period (11.5~13.5 dpc) of mouse inner ear development, *Pou3f4* expression is mainly detected in the area of otic capsule whereas in the later period (15.5~18.5 dpc), the expression pattern becomes restricted to the

cochlear lateral wall and spiral limbus area.[30] It seems that the temporal bone associated abnormalities assumed to be directly associated with the conductive component of hearing loss in DFN3 patients result from absence of functioning POU3F4 in earlier developmental periods of the inner ear. The sensorineural component of hearing loss in DFN3 patients is thought to be strongly correlated with the defects of the cochlear lateral wall, the development of which seems to require functioning POU3F4 in later developmental periods of the inner ear. In this study, we have focused on the role of POU3F4 in the development of cochlear lateral wall including the spiral ligament fibrocytes and stria vascularis both of which are essential for generation and maintenance of endocochlear potential.[31]

The 3 compartments of the cochlea are filled with 2 different types of fluids, the perilymph and endolymph, which have distinct electrolyte compositions.[54] The perilymph which fills the scala vestibule and scala tympani has low potassium and high sodium concentration resembling the extracellular fluid while the endolymph which bathes the apical surface of mechanosensory hair cells in the scala media, shows high potassium and low sodium concentration resembling the intracellular fluid.[54] These differences generate an endocochlear potential of approximately +80~100 mV that is required for the mechanosensory transduction in the cochlea.[54] The five types of spiral ligament fibrocytes each play specific roles in potassium recycling and the stria vascularis, a densely vascularized epithelium, provides the major driving force for generation of endocochlear potential.[31, 50, 54]

In this study, C3HeB/FeJ-*Pou3f4*$^{del\text{-}J}$/J, a mouse strain known to have spontaneous deletion of a segment encompassing the *Pou3f4* gene, was used for analysis of the role of Pou3f4.[40-41] This mutant mouse, found to have an approximately 550 kb sized deletion including *Pou3f4* according to genetic analysis, showed similar phenotypes as in human X-linked nonsyndromic hearing loss DFN3 including congenital deafness, defective modiolus, and

temporal bone abnormalities. In previous studies using other *Pou3f4*-deficient mouse models, defects of spiral ligament fibrocytes have been demonstrated in adult mutant mice.[16-17, 55-56] In contrast, stria vascularis have shown normal morphology in most reports although few studies reported detachment or missing stria vascularis in the mutants, which was assumed to be secondary to defects in the underlying fibrocytes.[16-17, 56] The mutant mouse used in this study also showed defects in all types of spiral ligament fibrocytes at P42 (Fig. 9). Type I, IV, V fibrocytes were almost completely lost and type II fibrocytes severely reduced. Type III fibrocytes showed normal differentiation up to P21 however failed to ultimately localize to the lining of otic capsule at final stages of differentiation (Fig. 10). Only few genes other than *Pou3f4* have been discovered to be associated with fibrocytes development including otospiralin (*Otos*) and *Tbx18*.[30, 57] Mice mutant for otospiralin (*Otos*), a gene encoding a small extracellular matrix protein of unknown function, were shown to have degeneration of type II and IV fibrocytes whereas *Tbx18*-mutants exhibited severe defects of otic fibrocytes together with almost complete absence of strial basal cells and a reduction of strial intermediate cells.[30, 57] We have found that the expression of *Tbx18* was unchanged in *Pou3f4*-deficient mice at E18.5 (data not shown) and also, normal expression of *Pou3f4* in *Tbx18*-mutants has already been previously reported,[30] which suggests these 2 transcriptional factors do not share a common genetic pathway regulating the differentiation of otic mesenchyme.

One of the novel findings of this study is the developmental defects of the stria vascularis caused by absence of functioning Pou3f4. Analysis of the developmental stages of the stria vascularis in *Pou3f4*-deficient mice revealed that *Pou3f4* is essential for timely cytodifferentiation of intermediate and basal cells of stria vascularis. The 3 cell types comprising the stria vascularis which include marginal, intermediate, and basal cells, all have different origins. Marginal cells are of epithelial origin and intermediate cells are differentiated

from neural crest origin cells while basal cells originate from the condensing mesenchymal cells of cochlear lateral wall.[30, 47] Considering that basal cells are differentiated from mesenchymal cells normally expressing *Pou3f4*, severe defect was expected in *Pou3f4*-deficient mice. Nevertheless, the basal cells eventually achieved normal differentiation although there is a time delay during the developmental process as shown in Fig. 12. As for the intermediate cells, the expression of Kir4.1 was significantly reduced at P42 despite the strong expression of *Trp2*,[49] a neural crest origin melanocyte marker, shown during the developmental process (Fig. 11). It seems that migration of neural crest-derived melanocytes occurs normally but further differentiation into functioning intermediate cells is blocked presumably due to delay in formation of intact basal cells resulting from absence of *Pou3f4*. Another possibility is that one of the downstream targets of *Pou3f4* may have a critical role in proper differentiation and survival of the intermediate cells. An interesting aspect is that the otic fibrocytes and basal cells of stria vascularis, both of which are derived from the mesenchymal cells normally expressing *Pou3f4* during development, showed different degree of requirement of *Pou3f4* in their differentiation process. Pou3f4 is absolutely required for proper differentiation of otic fibrocytes whereas condensation and differentiation of basal cells of stria vascularis can proceed without Pou3f4 function although slightly delayed.

From the results of this study, one of the mechanisms underlying the sensorineural hearing loss in DFN3 was found to be caused by compromise of cochlear lateral wall development including defects of both the otic fibrocytes and stria vascularis. In future studies, molecular networks regulating POU3F4 as well as downstream target genes of POU3F4 should be analyzed to better understand the precise roles of POU3F4 in normal inner ear patterning and the causative mechanism of DFN3.

# V. CONCLUSION

Five Korean families showing clinical characteristics of DFN3 were identified and genetic analysis revealed 5 different novel mutations in the *POU3F4* gene. To understand how these mutations affect the normal function of the POU3F4 protein, several molecular and cellular *in vitro* analyses were performed. Furthermore, using a mouse model for DFN3, the onset and pattern of the cochlear lateral wall abnormalities were studied in detail.

Protein modeling as well as *in vitro* assays demonstrated that the mutations identified in this study are detrimental to the tertiary structure of the POU3F4 protein and severely affect its ability to bind DNA. All three mutated POU3F4 proteins failed to transactivate expression of a reporter gene. In addition, all three failed to inhibit the transcriptional activity of wild type proteins when both wild type and mutant proteins were co-expressed. Our results strongly suggest that the deafness in DFN3 patients is largely due to the null function of POU3F4.

C3HeB/FeJ-*Pou3f4*$^{del\text{-}J}$/J analyzed in this study showed similar phenotype as in human X-linked nonsyndromic hearing loss DFN3 including congenital deafness, defective modiolus, and temporal bone abnormalities. Severe defects in all types of otic fibrocytes were identified in *Pou3f4*-deficient mice. Normal differentiation of the basal cells of stria vascularis could be achieved in the final stages without Pou3f4 function however the process was slightly delayed. Survival and differentiation of the strial intermediate cells were severely disrupted despite initial differentiation in the mutant mice.

Together, *in vitro* studies on novel mutations found in this study strongly suggest that the deafness in DFN3 patients is largely due to the null function of POU3F4 and animal study demonstrates that *POU3F4* mutation, leading to deafness in DFN3, causes severe developmental defects in the cochlear lateral wall including the otic fibrocytes and stria vascularis, both of which are

essential for ionic homeostasis and maintenance of endocochlear potential. Future analyses are required to discover the molecular networks regulating *POU3F4* as well as downstream target genes of *POU3F4* for better understanding of the precise roles of POU3F4 in normal inner ear patterning and the causative mechanism of DFN3.

REFERENCES


1. de Kok YJ, van der Maarel SM, Bitner-Glindzicz M, Huber I, Monaco AP, Malcolm S, et al. Association between X-linked mixed deafness and mutations in the POU domain gene POU3F4. Science 1995;267:685-8.
2. Bitner-Glindzicz M, Turnpenny P, Hoglund P, Kaariainen H, Sankila EM, van der Maarel SM, et al. Further mutations in Brain 4 (POU3F4) clarify the phenotype in the X-linked deafness, DFN3. Hum Mol Genet 1995;4:1467-9.
3. de Kok YJ, Cremers CW, Ropers HH, Cremers FP. The molecular basis of X-linked deafness type 3 (DFN3) in two sporadic cases: identification of a somatic mosaicism for a POU3F4 missense mutation. Hum Mutat 1997;10:207-11.
4. Friedman RA, Bykhovskaya Y, Tu G, Talbot JM, Wilson DF, Parnes LS, et al. Molecular analysis of the POU3F4 gene in patients with clinical and radiographic evidence of X-linked mixed deafness with perilymphatic gusher. Ann Otol Rhinol Laryngol 1997;106:320-5.
5. Cremers FP, Cremers CW, Ropers HH. The ins and outs of X-linked deafness type 3. Adv Otorhinolaryngol 2000;56:184-95.
6. Vore AP, Chang EH, Hoppe JE, Butler MG, Forrester S, Schneider MC, et al. Deletion of and novel missense mutation in POU3F4 in 2 families segregating X-linked nonsyndromic deafness. Arch Otolaryngol Head Neck Surg 2005;131:1057-63.
7. Wang QJ, Li QZ, Rao SQ, Zhao YL, Yuan H, Yang WY, et al. A novel mutation of POU3F4 causes congenital profound sensorineural hearing loss in a large Chinese family. Laryngoscope 2006;116:944-50.
8. de Kok YJ, Vossenaar ER, Cremers CW, Dahl N, Laporte J, Hu LJ, et al. Identification of a hot spot for microdeletions in patients with

X-linked deafness type 3 (DFN3) 900 kb proximal to the DFN3 gene POU3F4. Hum Mol Genet 1996;5:1229-35.

9. Arellano B, Ramirez Camacho R, Garcia Berrocal JR, Villamar M, del Castillo I, Moreno F. Sensorineural hearing loss and Mondini dysplasia caused by a deletion at locus DFN3. Arch Otolaryngol Head Neck Surg 2000;126:1065-9.

10. Nance WE, Setleff R, McLeod A, Sweeney A, Cooper C, McConnell F. X-linked mixed deafness with congenital fixation of the stapedial footplate and perilymphatic gusher. Birth Defects Orig Artic Ser 1971;07:64-9.

11. Phelps PD, Reardon W, Pembrey M, Bellman S, Luxom L. X-linked deafness, stapes gushers and a distinctive defect of the inner ear. Neuroradiology 1991;33:326-30.

12. Talbot JM, Wilson DF. Computed tomographic diagnosis of X-linked congenital mixed deafness, fixation of the stapedial footplate, and perilymphatic gusher. Am J Otol 1994;15:177-82.

13. Sennaroglu L, Sarac S, Ergin T. Surgical results of cochlear implantation in malformed cochlea. Otol Neurotol 2006;27:615-23.

14. Samadi DS, Saunders JC, Crenshaw EB, 3rd. Mutation of the POU-domain gene Brn4/Pou3f4 affects middle-ear sound conduction in the mouse. Hear Res 2005;199:11-21.

15. Cremers CW, Huygen PL. Clinical features of female heterozygotes in the X-linked mixed deafness syndrome (with perilymphatic gusher during stapes surgery). Int J Pediatr Otorhinolaryngol 1983;6:179-85.

16. Minowa O, Ikeda K, Sugitani Y, Oshima T, Nakai S, Katori Y, et al. Altered cochlear fibrocytes in a mouse model of DFN3 nonsyndromic deafness. Science 1999;285:1408-11.

17. Phippard D, Lu L, Lee D, Saunders JC, Crenshaw EB, 3rd. Targeted mutagenesis of the POU-domain gene Brn4/Pou3f4 causes

developmental defects in the inner ear. J Neurosci 1999;19:5980-9.

18. Herr W, Sturm RA, Clerc RG, Corcoran LM, Baltimore D, Sharp PA, et al. The POU domain: a large conserved region in the mammalian pit-1, oct-1, oct-2, and Caenorhabditis elegans unc-86 gene products. Genes Dev 1988;2:1513-6.
19. Klemm JD, Rould MA, Aurora R, Herr W, Pabo CO. Crystal structure of the Oct-1 POU domain bound to an octamer site: DNA recognition with tethered DNA-binding modules. Cell 1994;77:21-32.
20. Ryan AK, Rosenfeld MG. POU domain family values: flexibility, partnerships, and developmental codes. Genes Dev 1997;11:1207-25.
21. Hussain MA, Lee J, Miller CP, Habener JF. POU domain transcription factor brain 4 confers pancreatic alpha-cell-specific expression of the proglucagon gene through interaction with a novel proximal promoter G1 element. Mol Cell Biol 1997;17:7186-94.
22. Okazawa H, Imafuku I, Minowa MT, Kanazawa I, Hamada H, Mouradian MM. Regulation of striatal D1A dopamine receptor gene transcription by Brn-4. Proc Natl Acad Sci U S A 1996;93:11933-8.
23. Welter JF, Gali H, Crish JF, Eckert RL. Regulation of human involucrin promoter activity by POU domain proteins. J Biol Chem 1996;271:14727-33.
24. Hara Y, Rovescalli AC, Kim Y, Nirenberg M. Structure and evolution of four POU domain genes expressed in mouse brain. Proc Natl Acad Sci U S A 1992;89:3280-4.
25. Mathis JM, Simmons DM, He X, Swanson LW, Rosenfeld MG. Brain 4: a novel mammalian POU domain transcription factor exhibiting restricted brain-specific expression. Embo J 1992;11:2551-61.
26. Piussan C, Hanauer A, Dahl N, Mathieu M, Kolski C, Biancalana V, et al. X-linked progressive mixed deafness: a new microdeletion that involves a more proximal region in Xq21. Am J Hum Genet

1995;56:224-30.

27. Sennaroglu L, Saatci I. A new classification for cochleovestibular malformations. Laryngoscope 2002;112:2230-41.
28. Theiler K. The house mouse; development and normal stages from fertilization to 4 weeks of age. Berlin, New York,: Springer-Verlag; 1972.
29. Phippard D, Heydemann A, Lechner M, Lu L, Lee D, Kyin T, et al. Changes in the subcellular localization of the Brn4 gene product precede mesenchymal remodeling of the otic capsule. Hear Res 1998;120:77-85.
30. Trowe MO, Maier H, Schweizer M, Kispert A. Deafness in mice lacking the T-box transcription factor Tbx18 in otic fibrocytes. Development 2008;135:1725-34.
31. Kikuchi T, Adams JC, Miyabe Y, So E, Kobayashi T. Potassium ion recycling pathway via gap junction systems in the mammalian cochlea and its interruption in hereditary nonsyndromic deafness. Med Electron Microsc 2000;33:51-6.
32. Vriend G. WHAT IF: a molecular modeling and drug design program. J Mol Graph 1990;8:52-6, 29.
33. Chinea G, Padron G, Hooft RW, Sander C, Vriend G. The use of position-specific rotamers in model building by homology. Proteins 1995;23:415-21.
34. Hengen PN. Methods and reagents. Purification of GST fusion proteins. Trends Biochem Sci 1996;21:400-1.
35. Malik KF, Kim J, Hartman AL, Kim P, Young WS, 3rd. Binding preferences of the POU domain protein Brain-4: implications for autoregulation. Brain Res Mol Brain Res 1996;38:209-21.
36. Wang XH, Streeter M, Liu YP, Zhao HB. Identification and characterization of pannexin expression in the mammalian cochlea. J

Comp Neurol 2009;512:336-46.

37. Morsli H, Choo D, Ryan A, Johnson R, Wu DK. Development of the mouse inner ear and origin of its sensory organs. J Neurosci 1998;18:3327-35.

38. Cokol M, Nair R, Rost B. Finding nuclear localization signals. EMBO Rep 2000;1:411-5.

39. Reznikoff CA, Brankow DW, Heidelberger C. Establishment and characterization of a cloned line of C3H mouse embryo cells sensitive to postconfluence inhibition of division. Cancer Res 1973;33:3231-8.

40. Jones SM, Johnson KR, Yu H, Erway LC, Alagramam KN, Pollak N, et al. A quantitative survey of gravity receptor function in mutant mouse strains. J Assoc Res Otolaryngol 2005;6:297-310.

41. Nakano Y, Kim SH, Kim HM, Sanneman JD, Zhang Y, Smith RJ, et al. A claudin-9-based ion permeability barrier is essential for hearing. PLoS Genet 2009;5:e1000610.

42. Phippard D, Boyd Y, Reed V, Fisher G, Masson WK, Evans EP, et al. The sex-linked fidget mutation abolishes Brn4/Pou3f4 gene expression in the embryonic inner ear. Hum Mol Genet 2000;9:79-85.

43. Xia A, Kikuchi T, Hozawa K, Katori Y, Takasaka T. Expression of connexin 26 and Na,K-ATPase in the developing mouse cochlear lateral wall: functional implications. Brain Res 1999;846:106-11.

44. Li J, Verkman AS. Impaired hearing in mice lacking aquaporin-4 water channels. J Biol Chem 2001;276:31233-7.

45. Ando M, Takeuchi S. Immunological identification of an inward rectifier K+ channel (Kir4.1) in the intermediate cell (melanocyte) of the cochlear stria vascularis of gerbils and rats. Cell Tissue Res 1999;298:179-83.

46. Kitajiri S, Miyamoto T, Mineharu A, Sonoda N, Furuse K, Hata M, et al. Compartmentalization established by claudin-11-based tight

junctions in stria vascularis is required for hearing through generation of endocochlear potential. J Cell Sci 2004;117:5087-96.

47. Steel KP, Barkway C. Another role for melanocytes: their importance for normal stria vascularis development in the mammalian inner ear. Development 1989;107:453-63.

48. Birkenhager R, Otto E, Schurmann MJ, Vollmer M, Ruf EM, Maier-Lutz I, et al. Mutation of BSND causes Bartter syndrome with sensorineural deafness and kidney failure. Nat Genet 2001;29:310-4.

49. Steel KP, Davidson DR, Jackson IJ. TRP-2/DT, a new early melanoblast marker, shows that steel growth factor (c-kit ligand) is a survival factor. Development 1992;115:1111-9.

50. Takeuchi S, Ando M, Kakigi A. Mechanism generating endocochlear potential: role played by intermediate cells in stria vascularis. Biophys J 2000;79:2572-82.

51. Hagiwara H, Tamagawa Y, Kitamura K, Kodera K. A new mutation in the POU3F4 gene in a Japanese family with X-linked mixed deafness (DFN3). Laryngoscope 1998;108:1544-7.

52. Lee HK, Lee SH, Lee KY, Lim EJ, Choi SY, Park RK, et al. Novel POU3F4 mutations and clinical features of DFN3 patients with cochlear implants. Clin Genet 2009;75:572-5.

53. Petersen MB, Wang Q, Willems PJ. Sex-linked deafness. Clin Genet 2008;73:14-23.

54. Wangemann P. Supporting sensory transduction: cochlear fluid homeostasis and the endocochlear potential. J Physiol 2006;576:11-21.

55. Xia AP, Kikuchi T, Minowa O, Katori Y, Oshima T, Noda T, et al. Late-onset hearing loss in a mouse model of DFN3 non-syndromic deafness: morphologic and immunohistochemical analyses. Hear Res 2002;166:150-8.

56. Braunstein EM, Crenshaw Iii EB, Morrow BE, Adams JC. Cooperative

Function of Tbx1 and Brn4 in the Periotic Mesenchyme is Necessary for Cochlea Formation. J Assoc Res Otolaryngol 2008;9:33-43.

57. Delprat B, Ruel J, Guitton MJ, Hamard G, Lenoir M, Pujol R, et al. Deafness and cochlear fibrocyte alterations in mice deficient for the inner ear protein otospiralin. Mol Cell Biol 2005;25:847-53.

< ABSTRACT(IN KOREAN)>

# 비증후군성 유전성 난청 DFN3 환자들에서 발견된 새로운 *POU3F4* 유전자 변이에 대한 임상적 및 분자생물학적 분석과 내이 발생에 있어서 POU3F4의 역할

<지도교수 이원상>

연세대학교 대학원 의학과

송 미 현

X-유전 비증후군성 난청 DFN3는 X 염색체로 유전되는 난청 중 가장 흔한 형태로 POU family의 전사인자 중 하나를 발현하는 *POU3F4* 유전자의 변이에 의해 발생한다. DFN3에서 일반적으로 관찰되는 선천성 난청과 특징적 내이 기형을 가진 한국인 다섯 가족을 대상으로 한국인에 특징적인 새로운 *POU3F4* 유전자 변이를 발견하기 위해 유전자 분석을 시행하였다. 본 연구에서는 새롭게 발견된 유전자 변이가 정상적인 POU3F4 기능에 어떠한 영향을 미치는지를 알아보기 위하여 분자생물학적 *in vitro* 분석을 시행하였다. 또한 DFN3의 동물 모델을 이용하여 내이발생 과정에서 POU3F4의 역할에 대하여 알아보았다.

DFN3 한국인 다섯 가족에서 유전자 분석을 시행하였으며 모든 가족에서 새로운 *POU3F4* 유전자 변이가 발견되었다. 세 가족에서는 *POU3F4* 유전자 내에서 변이가 발견되었는데 p.R329P, p.S310del, 그리고 p.Ala116fs의 각각 다른 종류의 변이를 보였다. 두 가족에서는 *POU3F4* 유전자 전체 및 그 주변을 포함하는 deletion 변이가 발견되었고 그 중 하나는 *POU3F4* 유전자의 조절인자가 존재하는 것으로 알려진 유전자 앞쪽 부위의 deletion이었고 다른 하나는 *POU3F4* 유전자를 포함한 Xq21 부위 거의 전체가 삭제된 큰 deletion 변이였다.

본 연구에서 발견된 유전자 변이 중 *POU3F4* 유전자 내의 변이 3

종류를 대상으로 추가적인 분자생물학적 분석을 진행하였다. 컴퓨터를 이용한 단백질의 삼차원적 구조 분석과 EMSA 분석을 통하여 3종류의 변이 모두 POU3F4 단백질의 삼차원적 구조를 변형시키며 이로 인하여 DNA에 결합하는 능력이 거의 소실되는 것을 알 수 있었다. 또한 변이된 POU3F4 단백질 모두 전사 활성자로서의 기능이 소멸되었고 정상적인 단백질과 변이 단백질을 동시에 발현시켰을 때 변이 단백질이 정상 단백질의 전사 기능에 영향을 미치지 못하였다.

DFN3의 동물 모델인 Pou3f4$^{del-J}$를 이용하여 분석한 결과 이 모델은 사람에서의 DFN3의 임상적 특징을 잘 반영하는 것으로 나타났다. 내이의 발생 과정 중 *Pou3f4*가 와우의 외측 벽에 발현하는 것을 고려하여 *Pou3f4* 변이 동물에서 내이 발생에 어떠한 이상이 생기는지를 알아보았다. 와우 외측 벽의 구조인 나선인대 섬유질 세포(otic fibrocyte)와 혈관조(stria vascularis)를 면역조직화학염색과 *in-situ* hybridization 분석을 통하여 살펴보았을 때 모든 종류의 나선인대 섬유질 세포가 정상적인 분화되지 못하였고 혈관조에 있어서는 기저세포(basal cell)는 정상적인 분화를 보이지만 그 과정이 지연되었고 중간세포(intermediate cell)는 초기에는 분화를 하지만 최종적으로는 정상 생존 및 분화가 이루어지지 못하는 것으로 나타났다.

결론적으로 본 연구에서는 DFN3 한국인 가족에서 5 종류의 새로운 *POU3F4* 유전자 변이가 발견되었고 이러한 변이는 POU3F4의 전사인자로서의 기능을 소멸시킴으로써 DFN3에서의 내이 기형 및 난청을 유발하였다. 동물 실험을 통하여 Pou3f4가 와우 외측 벽의 발생에 중요한 역할을 하며 Pou3f4 기능이 없는 경우 와우 내의 이온 항상성과 와우내전위 유지에 중요한 역할을 하는 섬유질 세포와 혈관조에 이상이 생겨 DFN3에서 난청이 유발됨을 알 수 있었다.

---

핵심되는 말 : 난청, DFN3, POU3F4, 내이 발생